Negative Thermal Expansion in the Mixed Valence Ytterbium Fulleride, $Yb_{2.75}C_{60}$

Serena Margadonna,*,† J. Arvanitidis,‡ Konstantinos Papagelis,‡ and Kosmas Prassides*,‡

School of Chemistry, University of Edinburgh, Edinburgh EH9 3JJ, United Kingdom, and Department of Chemistry, University of Durham, Durham DH1 3LE, United Kingdom

Received June 22, 2005

The powder synchrotron X-ray diffraction technique was used to study the temperature evolution of the structural properties of the mixed valence rare earth fulleride, $Yb_{2.75}C_{60}$, in the temperature range 5−295 K. The large lattice expansion (negative thermal expansion) on cooling below 60 K provides an unambiguous signature of a temperature-induced valence transition of the Yb atoms. The transformation is of electronic origin and is driven by the coupling of the Yb 4f band and the t_{1u} band of C_{60}. It is analogous to that observed at lower temperatures in $Sm_{2.75}C_{60}$, but it is absent when the electronically active 4f sublattice is missing in the related alkaline earth fulleride, $Ca_{2.75}C_{60}$.

Introduction

The chemistry of the rare earth elements is typically dominated by the +3 oxidation state. Well-established exceptions include Ce, Sm, Eu, Tm, and Yb compounds, in which the +4 or +2 oxidation states can be also stabilized. Of particular interest in such circumstances are selected rare earth systems (Kondo insulators, heavy fermions) for which the 4f levels lie close to the Fermi level, E_F, and may exhibit the phenomenon of intermediate valence (IV).[1] The ground state of IV solids such as SmS, SmB_6, and YbB_{12} has been rationalized phenomenologically in terms of the valence fluctuation model of two nearly degenerate electronic configurations, $4f^n5d^0$ and $4f^{n-1}5d^1$. The hybridization strength between the localized 4f and the conduction 5d electrons can be tuned both by chemical substitution and by the application of pressure.[2−6] Unambiguous signatures of electronically driven valence changes with changes in external stimuli (temperature, pressure) are found in the variation of the elastic properties of IV solids: anomalous expansion coefficients without an accompanying change in crystal structure can be attributed to the differing radii of the rare earth $4f^n$ and $4f^{n-1}$ states. Of particular importance in this field will be examples of IV solids in which the strongly correlated rare earth cation sublattice is combined with an electronically active anion sublattice. For instance, the $YbGa_{1+x}Ge_{1-x}$ intermetallic system exhibits both continuous[7] and abrupt[8] temperature-induced $Yb^{(2+\epsilon)+} \rightarrow Yb^{2+}$ valence changes, which are controlled by the spilling over of Ga 4p electronic density into the Yb 4f band and manifest themselves in zero (ZTE) and negative (NTE) thermal expansion coefficients, respectively.

The fullerene solid-state chemistry of the rare earths has not been explored in a systematic way principally because of the difficulties in devising reliable protocols for preparation of single-phase materials; reactions of rare earth metals with fullerenes require high temperature and under these conditions, formation of rare earth carbides competes with that of fullerides. This is despite the possibility that molecular materials with novel electronic and magnetic properties may be isolated when the metal dopants in fulleride salts are electronically active and carry a magnetic moment unlike the well-studied cases of alkali and alkaline earth fullerides. For instance, exploration of the phase diagram of $Eu-C_{60}$ and $-C_{70}$ has led to the isolation of molecular ferromagnets,[9−11] which exhibit metallic and negative magnetoresistive behavior with magnetic correlations developing either through direct exchange interactions between the rare earths ions or through π-d,f interactions modulated by C_{60}. In addition, there have been early reports of superconducting rare earth fulleride phases with the chemical formula $RE_{2.75}C_{60}$ (RE = Yb, Sm) and $T_c \sim 6$ K and 8 K, respectively.[12,13]

* Authors to whom correspondence should be addressed. E-mail: serena.margadonna@ed.ac.uk (S.M.); K.Prassides@durham.ac.uk (K.P.).
† University of Edinburgh.
‡ University of Durham.

(1) Wachter, P. In *Handbook on the Physics and Chemistry of Rare Earths*; Gschneidner, K. A., Eyring, L., Lander, G. H., Chopin, G. R., Eds.; North-Holland: Amsterdam, 1994; Vol. 19, p 177.
(2) Jayaraman, A.; Bucher, E.; Dernier, P. D.; Longinotti, L. D. *Phys. Rev. Lett.* **1973**, *31*, 700.
(3) Jayaraman, A.; Narayanamurti, V.; Bucher, E.; Maines, R. G. *Phys. Rev. Lett.* **1970**, *25*, 1430.
(4) Lawrence, J. M.; Kwei, G. H.; Sarrao, J. L.; Fisk, Z.; Mandrus, D.; Thompson, J. D. *Phys. Rev. B* **1996**, *54*, 6011.
(5) Dallera, C.; Grioni, M.; Shukla, A.; Vanko, G.; Sarrao, J. L.; Rueff, J.-P.; Cox, D. L. *Phys. Rev. Lett.* **2002**, *88*, 196403.
(6) Barla, A.; Sanchez, J. P.; Haga, Y.; Lapertot, G.; Doyle, B. P.; Leupold, O.; Ruffer, R.; Abd-Elmeguid, M. M.; Lengsdorf, R.; Flouquet, J. *Phys. Rev. Lett.* **2004**, *92*, 066401.
(7) Salvador, J. R.; Guo, F.; Hogan, T.; Kanatzidis, M. G. *Nature* **2003**, *425*, 702.
(8) Margadonna, S.; Prassides, K.; Fitch, A. N.; Salvador, J. R.; Kanatzidis, M. G. *J. Am. Chem. Soc.* **2004**, *126*, 4498.
(9) Ishii, K.; Fujiwara, A.; Suematsu, H.; Kubozono, Y. *Phys. Rev. B* **2002**, *65*, 134431.
(10) Margiolaki, I.; Margadonna, S.; Prassides, K.; Hansen, T.; Ishii, K.; Suematsu, H. *J. Am. Chem. Soc.* **2002**, *124*, 11288.
(11) Takenobu, T.; Chi, D. H.; Margadonna, S.; Prassides, K.; Kubozono, Y.; Fitch, A. N.; Kato, K.; Iwasa, Y. *J. Am. Chem. Soc.* **2003**, *125*, 1897.
(12) Özdas, E.; Kortan, A. R.; Kopylov, N.; Ramirez, A. P.; Siegrist, T.; Rabe, K. M.; Bair, H. E.; Schuppler, S.; Citrin, P. H. *Nature* **1995**, *375*, 126.
(13) Chen, X. H.; Roth, G. *Phys. Rev. B* **1995**, *52*, 15534.

10.1021/cm051341k CCC: $30.25
Published on Web 08/04/2005

While the report of superconductivity in $Sm_{2.75}C_{60}$ has now been shown to be erroneous,[14,15] our recent work has also established that remarkably $Sm_{2.75}C_{60}$ displays both temperature-induced $Sm^{(2+\epsilon)+} \rightarrow Sm^{2+}$ (at 32 K)[14] and pressure-induced $Sm^{(2+\epsilon)+} \rightarrow Sm^{3+}$ (at 4 GPa)[16] valence transitions, accompanied by dramatic isosymmetric lattice responses—negative thermal expansion and volume collapse, respectively. These effects are unprecedented in fullerene (or other molecular) systems and establish an unexpected link to the class of strongly correlated Kondo systems, which currently attracts broad experimental and theoretical interest. The availability of the narrow C_{60} t_{1u} band with its unconventional strongly correlated character[17−20] in close proximity to the rare earth 4f and 5d bands makes $Sm_{2.75}C_{60}$ particularly intriguing when compared with other known Kondo insulators such as the samarium chalcogenides, which comprise closed-shell anionic sublattices.

Here, we report the results of multitemperature synchrotron X-ray diffraction experiments on the related rare earth fulleride $Yb_{2.75}C_{60}$ between 295 and 5 K. The temperature evolution of the lattice parameters is a powerful and direct indicator of what is happening in the material at the microscopic level. We observe a sudden change in the sign of the thermal expansivity that becomes very large and negative on cooling below 60 K, thereby reflecting a change in size of the Yb ions, which in turn can be directly related to a temperature-induced change in their valence state.

Experimental Methods

Synthesis. $Yb_{2.75}C_{60}$ samples were prepared by reaction of stoichiometric quantities of C_{60} and Yb pressed into pellets and contained in a sealed tantalum cell inside an evacuated quartz tube at 620 °C for a total time of 6.5 h with two intermediate grindings. The pellets were then cooled to room temperature in 5−6 h. Phase purity was confirmed by X-ray diffraction with a Siemens D5000 diffractometer.

Structure Analysis. For the synchrotron X-ray diffraction measurements, the samples were sealed in thin-wall capillaries 0.5 mm in diameter. Diffraction data ($\lambda = 0.85066$ Å) were collected on heating between 5 and 295 K (using a continuous-flow cryostat) in continuous scanning mode using nine Ge(111) analyzer crystals with the high-resolution powder diffractometer on beamline ID31, European Synchrotron Radiation Facility (ESRF), Grenoble. The data were rebinned to a step of 0.005° in the range 3.5−31.5°. Data analysis was performed with the GSAS suite of Rietveld analysis programs.[21] Some impurity peaks were excluded from the refinements.

Magnetic Measurements. Total susceptibilities were measured for $Yb_{2.75}C_{60}$ samples ($m \sim 125$ mg) between 2 and 300 K in a field of 1 T after correcting for the diamagnetic core contributions with a Quantum Design MPMS5 SQUID susceptometer. Low-field measurements reveal that $Yb_{2.75}C_{60}$ does not display bulk superconductivity down to 2 K in contrast to earlier reports.[12]

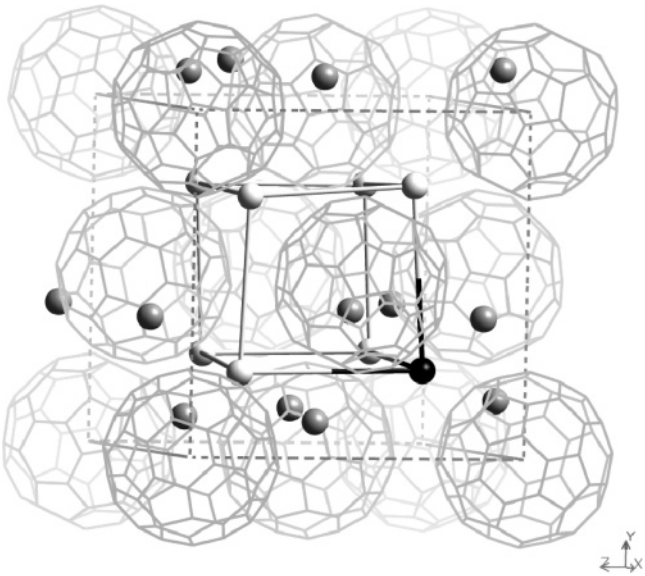

Figure 1. Building block of the orthorhombic superstructure of $Yb_{2.75}C_{60}$ that can be obtained by doubling the subcell along all three lattice directions. Distorted octahedral and tetrahedral ytterbium cations are depicted as dark and light gray spheres, respectively. The tetrahedral ytterbium defect is shown as black spheres.

Table 1. Refined Structural Parameters for $Yb_{2.75}C_{60}$ Obtained from the Rietveld Refinement of the Synchrotron X-ray Diffraction Data at 5 K

	structural parameters					
	site	*x*/*a*	*y*/*b*	*z*/*c*	N	*B* (Å^2)
C_{60}(1)	4*a*	0	0	0	1.0	1.0(1)
C_{60}(21)	8*c*	0	1/4	1/4	1.0	1.0(1)
C_{60}(22)	8*c*	1/4	0	1/4	1.0	1.0(1)
C_{60}(23)	8*c*	1/4	1/4	0	1.0	1.0(1)
C_{60}(3)	4*b*	1/2	1/2	1/2	1.0	1.0(1)
Yb(11)	8*c*	0.1351(3)	0.1150(3)	0.3834(3)	0.983(1)	2.6(1)
Yb(12)	8*c*	0.3834(3)	0.1351(3)	0.1150(3)	0.983(1)	2.6(1)
Yb(13)	8*c*	0.1150(3)	0.3834(3)	0.1351(3)	0.983(1)	2.6(1)
Yb(21)	8*c*	0.1322(3)	0.3694(3)	0.3768(4)	0.983(1)	2.6(1)
Yb(22)	8*c*	0.3768(4)	0.1322(3)	0.3694(3)	0.983(1)	2.6(1)
Yb(23)	8*c*	0.3694(3)	0.3768(4)	0.1322(3)	0.983(1)	2.6(1)
Yb(3)	8*c*	0.379(1)	0.380(1)	0.373(1)	0.983(1)	2.6(1)
Yb(4) (vacancy)	8*c*	0.121(1)	0.120(1)	0.127(1)	0.115(7)	2.6(1)
Yb(51)	8*c*	0.20087(9)	0.20087(9)	0.20087(9)	0.927(2)	0.9(1)
Yb(52)	8*c*	0.04913(9)	0.04913(9)	0.20087(9)	0.927(2)	0.9(1)
Yb(53)	8*c*	0.20087(9)	0.04913(9)	0.04913(9)	0.927(2)	0.9(1)
Yb(54)	8*c*	0.04913(9)	0.20087(9)	0.04913(9)	0.927(2)	0.9(1)
Yb(61)	8*c*	0.19019(9)	0.309(1)	0.309(1)	0.073(2)	0.9(1)
Yb(62)	8*c*	0.05989(9)	−0.0590(1)	0.309(1)	0.073(2)	0.9(1)
Yb(63)	8*c*	0.309(1)	−0.059(1)	0.060(1)	0.145(5)	0.9(1)

Results and Discussion

The structural properties of $Yb_{2.75}C_{60}$ were studied as a function of temperature between 5 and 295 K by high-resolution synchrotron X-ray powder diffraction. Rietveld refinement of an extended *Q*-range diffraction data set at 5 K proceeded smoothly with the structural model (Figure 1, space group *Pcab*, option 2)[12,14] of $Sm_{2.75}C_{60}$ ($a = 27.9338(6)$ Å, $b = 27.9733(8)$ Å, $c = 27.9063(6)$ Å, agreement factors: $R_{wp} = 4.86\%$, $R_{exp} = 1.59\%$, Table 1, Figure 2). As in $Sm_{2.75}C_{60}$, the observed superstructure in $Yb_{2.75}C_{60}$ arises from long-range ordering of tetrahedral Yb defects, namely, one out of every eight tetrahedral sites is only

(14) Arvanitidis, J.; Papagelis, K.; Margadonna, S.; Prassides, K.; Fitch, A. N. *Nature* **2003**, *425*, 599.
(15) Claves, D.; Hamwi, A. *Solid State Commun.* **2000**, *113*, 357.
(16) Arvanitidis, J.; Papagelis, K.; Margadonna, S.; Prassides, K. *Dalton Trans.* **2004**, 3144.
(17) Margadonna, S.; Prassides, K. *J. Solid State Chem.* **2002**, *168*, 639.
(18) Durand, P.; Darling, G. R.; Dubitsky, Y.; Zaopo, A.; Rosseinsky, M. J. *Nat. Mater.* **2003**, *2*, 605.
(19) Gunnarsson, O. *Alkali-Doped Fullerides*; World Scientific: Singapore, 2004.
(20) Margadonna, S.; Iwasa, Y.; Takenobu, T.; Prassides, K. *Struct. Bonding* **2004**, *109*, 127.
(21) Larsen, A. C.; von Dreele R. B. *GSAS software*; Los Alamos National Laboratory Report No. LAUR 86−748.

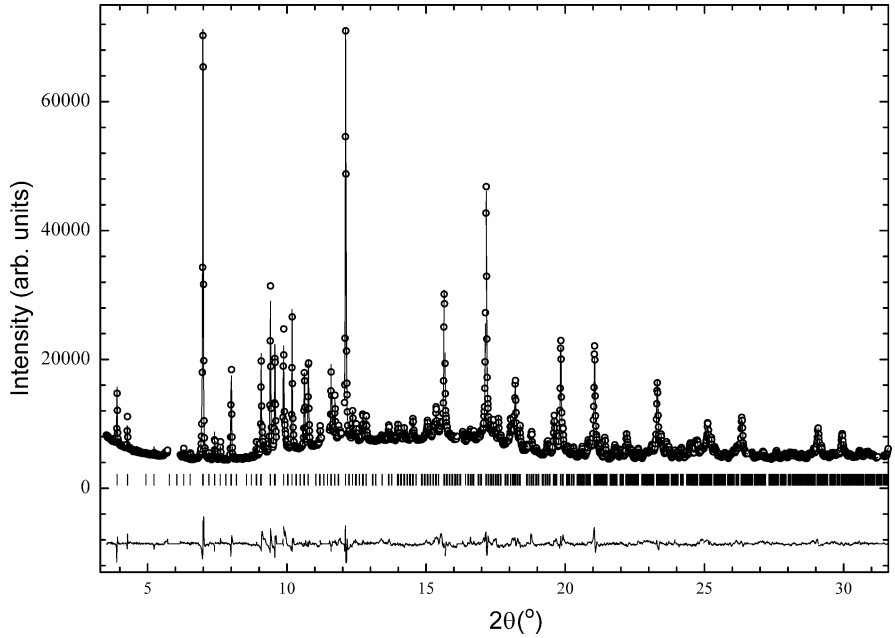

Figure 2. Final observed (○) and calculated (solid line) synchrotron X-ray powder (λ = 0.85066 Å) diffraction profiles for $Yb_{2.75}C_{60}$ at 5 K. The lower solid line shows the difference profile and the tick marks show the reflection positions. Some impurity peaks were excluded from the refinement.

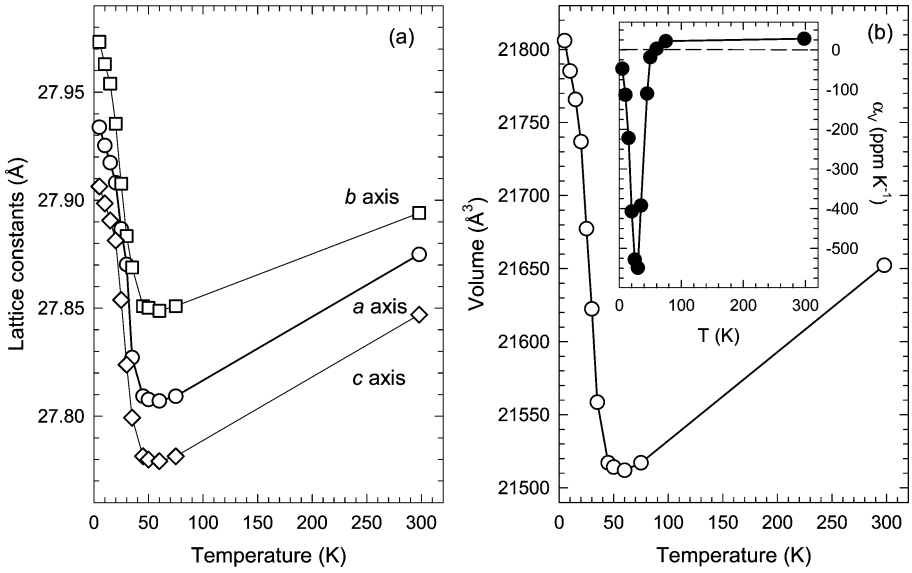

Figure 3. Temperature evolution of (a) the orthorhombic lattice constants *a* (○), *b* (□), and *c* (◇) and (b) unit cell volume in $Yb_{2.75}C_{60}$. The inset in b shows the temperature dependence of the coefficient of thermal expansion, $\alpha_V = \mathrm{d} \ln V/\mathrm{d}T$.

partially occupied. Long-range ordering of these defects (their Yb fractional occupancy converging to ~12% in the present refinement) results in a unit cell with dimensions twice as large as those of the fcc alkali fullerides. In the course of the refinements, the shape of the C_{60} molecules was constrained to icosahedral symmetry with a cage diameter of 7.01 Å, and all C−C bond lengths were fixed to a value of 1.44 Å. Two hundred forty independent C atoms were needed to define the 32 C_{60} molecules present in the unit cell. The five symmetry-inequivalent C_{60} molecules in the unit cell, $C_{60}(1)$ at (000), $C_{60}(21)$ at ($0^1/_4{}^1/_4$), $C_{60}(22)$ at ($^1/_4 0^1/_4$), $C_{60}(23)$ at ($^1/_4{}^1/_4 0$), and $C_{60}(3)$ at ($^1/_2{}^1/_2{}^1/_2$), were rotated anticlockwise by 37.5° about their local [111], [$1\bar{1}\bar{1}$], [$\bar{1}1\bar{1}$], [$\bar{1}\bar{1}1$], and [111] symmetry axes, respectively. This orientational arrangement of the C_{60} units (different from that proposed in ref 12) leads to improved agreement factors for the Rietveld refinement and avoids unphysically short Yb−C_{60} contacts. In the refined structural model, the Yb cations are displaced from the centers of the octahedral sites by ~2.4 Å and from the centers of the tetrahedral sites by ~0.3 Å with a shortest Yb(3)−C_{60} contact of 2.64(3) Å.

However, a striking feature of the temperature dependence of the diffraction data is that the angular positions of the diffraction peaks shift significantly to higher values as the temperature increases toward 60 K, implying an anomalous structural behavior whereby the unit cell metrics decrease continuously with increasing temperature. Extraction of reliable lattice constants (Figure 3a) was performed with the LeBail pattern decomposition technique using the same orthorhombic model at all temperatures. The temperature evolution of the extracted unit cell volume is shown in Figure 3b. The thermal expansivity α_V (=d ln *V*/d*T*) is negative throughout this temperature range. It first increases in absolute value continuously on heating until it goes through

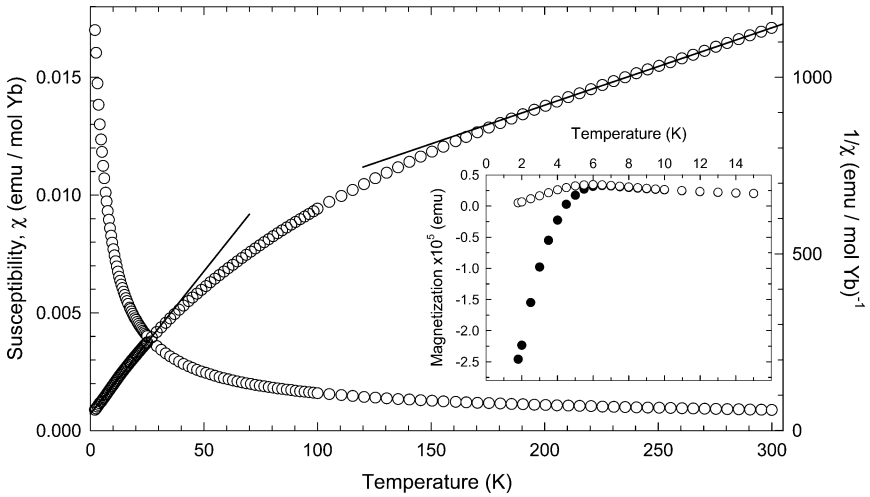

Figure 4. Temperature dependence of the magnetic susceptibility, χ (left scale), and its reciprocal, $1/\chi$ (right scale, $H = 1$ T), for $Yb_{2.75}C_{60}$. The straight lines depict Curie−Weiss fits of the inverse susceptibility data in the ranges 200−300 K and 2−35 K. The inset shows the temperature dependence of the ZFC (full circles) and FC (open circles) magnetization in a field of 5 Oe.

a maximum of −550 ppm/K at 30 K and then rapidly approaches zero at ∼60 K (Figure 3b inset). This behavior leads to an overall decrease in lattice size of 1.4% on heating from 5 to 60 K with no observable change in crystal symmetry. However, the widths of the diffraction peaks also vary in the temperature range in which the negative thermal expansion is observed, going through a maximum (larger by ∼40% than the average value) at the same temperature (30 K) at which the rate of change in lattice size is maximal. Such behavior most likely reflects the presence of local structural inhomogeneities accompanying the rapid transformation of the material.

The anomalous lattice response disappears above 60 K (Figure 3), and the lattice constants increase on heating to 295 K, resulting in an overall volume expansion at a rate of ∼28 ppm K^{-1}, comparable to what is normally expected for a metal fulleride solid. Nonetheless, it is remarkable that the lattice expansion in the high-temperature regime is still not large enough to produce a cell volume at ambient temperature comparable to that at 5 K.

Variable-temperature magnetic susceptibility measurements at 1 T showed that the Curie−Weiss law was obeyed only over a restricted temperature range, ∼200−300 K with $\mu_{eff} = 1.9\ \mu_B$ per Yb ion and $\Theta = 220$ K (Figure 4). As Yb^{3+} is paramagnetic with a calculated free-ion effective magnetic moment of 4.54 μ_B and Yb^{2+} is diamagnetic, we can obtain an estimate of the average Yb oxidation state in $Yb_{2.75}C_{60}$ as approximately equal to +2.18, assuming that the measured susceptibility is the sum of the Yb^{2+} and Yb^{3+} susceptibilities, weighted by their relative concentration. Below 200 K, $\chi^{-1}(T)$ strongly deviates from linearity as crystal field effects associated with the splitting of the $^2F_{7/2}$ octet ground-state term of Yb^{3+} set in. Nonetheless, Curie−Weiss behavior is also observed below 35 K with a reduced magnetic moment of 1.0 μ_B per Yb ion, much lower than expected from CF effects alone. Though the influence of the ligand field on the magnetism of Yb^{3+} complicates unambiguous assignment, the reduced average Yb valence of +2.05 at low T is consistent with a temperature-induced valence change on cooling.

Therefore, the anomalous response of the $Yb_{2.75}C_{60}$ lattice size at low temperature without an accompanying change in crystal symmetry can be rationalized in terms of the average Yb oxidation state approaching +2 upon cooling below ∼60 K. As the valence decreases from +2.18, the Yb ionic radius increases continuously and the material displays a negative thermal expansion (NTE) coefficient, which is maximal at ∼30 K with a value of −550 ppm/K, somewhat smaller than that encountered in $Sm_{2.75}C_{60}$ (−1000 ppm/K)[14] but considerably larger than those in NTE framework oxide materials such as ZrW_2O_8 (−27 ppm/K).[22] The large magnitude of the volume inflation (∼1.4%), even larger than that of ∼0.8% in $Sm_{2.75}C_{60}$, despite the small rare earth valence change (∼0.13) implied by the magnetic susceptibility data may be understood if we note that the tetrahedral hole in $Yb_{2.75}C_{60}$ has a radius of 1.12 Å, straddling the values of the ionic radii of Yb^{2+} (1.16 Å) and Yb^{3+} (1.01 Å), and therefore, even small changes in valence have a profound effect on lattice size. We also propose that the driving force of the valence change is *electronic* in origin and is inherently connected with the details of the density of states of these systems, shown schematically in Figure 5. At high temperatures, 4f electrons can be thermally excited from the narrow 4f band into the C_{60} t_{1u} band; the latter becomes full with six electrons when the Yb valence approaches +2.18. At low temperatures, these electrons are taken back into the 4f band resulting in a $4f^{14}$ Yb electronic configuration and an expanded ionic radius. Consistent with this picture, the isoelectronic and isostructural $Ca_{2.75}C_{60}$ fulleride[23] which lacks an electronically active 4f sublattice shows no anomalous expansion behavior, its lattice contracting between 295 and 5 K by ∼0.4%.

A prominent feature of the present results is that the average rare earth valences at high temperature are essentially identical for both $Yb_{2.75}C_{60}$ and $Sm_{2.75}C_{60}$ at ca. +2.2. This can be rationalized if we note that it corresponds to full occupation of the LUMO t_{1u}-derived band of the fullerene

(22) Evans, J. S. O. *J. Chem. Soc., Dalton Trans*. **1999**, 3317.
(23) Claridge, J. B.; Kubozono, Y.; Rosseinsky, M. J. *Chem. Mater*. **2003**, *15*, 1830.

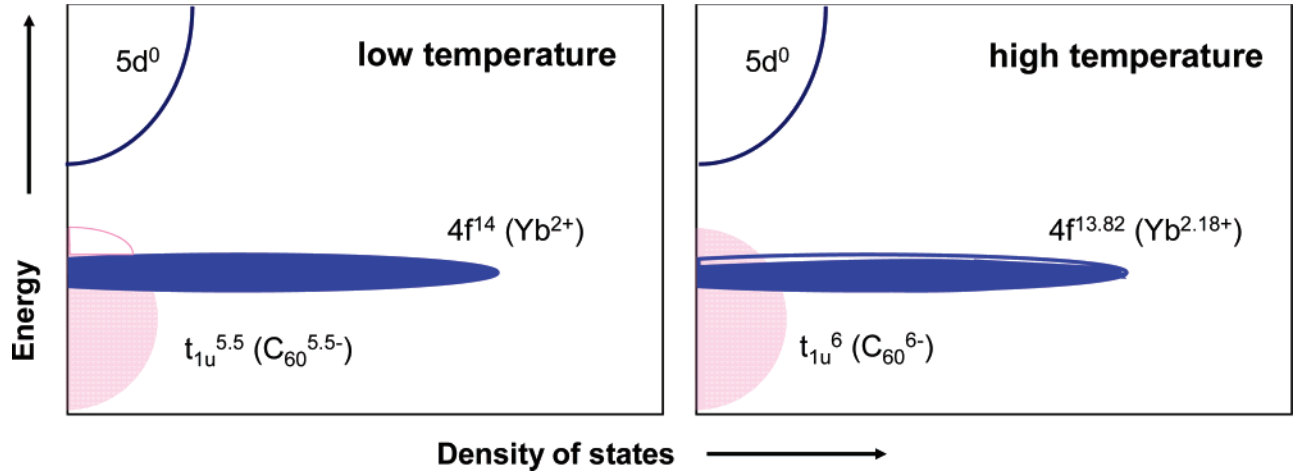

Figure 5. Schematic representation of the electronic density of states in $Yb_{2.75}C_{60}$ at low and high temperature, showing the spilling over of electron density from the Yb 4f band to the t_{1u} band of C_{60} on heating.

units and a formal charge of −6 for the fulleride sublattice. Then, the rare observation that temperature-induced valence transitions can occur for the same Yb and Sm compounds implies that the electronically active t_{1u} band of C_{60} plays an important role in defining the electronic properties of these systems; this is in contrast to the usual situation in intermediate valence rare earth solids whence the anionic sublattice is closed-shell electronically inactive and plays little role in determining the electronic properties. Thus, we may confidently predict that analogous electronic and structural instabilities should be also encountered for other isostructural and isoelectronic rare earth fullerides (e.g., $Eu_{2.75}C_{60}$, $Tm_{2.75}C_{60}$). Moreover, as changing the nature of the rare earth cation sublattice from Sm to Yb sensitively affects the onset temperature of the negative thermal expansion behavior, which increases significantly from 32 to 60 K, detailed exploration of the phase diagram of binary and ternary rare earth fulleride salts could allow us to drive the occurrence of such phenomena to even higher temperatures.

Finally, we comment on the results of low-field (5 Oe) zero-field-cooled (ZFC) and field-cooled (FC) magnetization measurements on $Yb_{2.75}C_{60}$. Such measurements were performed on many different batches, which exhibited essentially identical powder X-ray diffraction patterns. In some cases, a very small diamagnetic response with an onset at ∼6 K was observed. The data for a sample that showed the maximum field expulsion is shown as an inset in Figure 4. While the observed onset coincides with that reported earlier in ref 12, our data do not support the presence of bulk superconductivity in $Yb_{2.75}C_{60}$ as the maximum superconducting fraction that is calculated is less than 0.8%. We stress that in our analogous measurements on $Sm_{2.75}C_{60}$,[14] trace superconductivity was never observed for any of the numerous samples studied. This implies that a superconducting ytterbium fulleride may be indeed present in the Yb−C_{60} phase field, but it still remains to be identified. Given that $Yb_{2.75}C_{60}$ is a member of a family of $Yb_{3-x}C_{60}$ phases with variable defect content x, superconductivity may be encountered for a value of x different from 0.25. Alternatively, taking into account our knowledge of the chemistry of alkaline earth fullerides where superconductivity is found for compositions with stoichiometry AE_4C_{60} (AE = Ba, Sr),[24] an analogous Yb_4C_{60} phase is indeed expected to display superconducting properties.[25]

Conclusion

In conclusion, $Yb_{2.75}C_{60}$ shows on cooling a temperature-induced quasi-continuous isosymmetric phase transformation to a significantly expanded lattice. The transition is of electronic origin, driven by the $Yb^{2+} \leftrightarrow Yb^{3+} + e$ electron transfer and the coupling of the Yb 4f band to the electronically active t_{1u} band of C_{60}. The NTE behavior is found at a substantially higher temperature (∼60 K) than in $Sm_{2.75}C_{60}$ (32 K) and is absent in the lattice response of the related alkaline earth fulleride $Ca_{2.75}C_{60}$.

Acknowledgment. We thank the EPSRC for financial support, the ESRF for provision of synchrotron X-ray beamtime, the Royal Society for a Dorothy Hodgkin Research Fellowship (S.M.), Dr. Andrew N. Fitch (ESRF) for help with the experiments, and Prof. Y. Kubozono (Okayama University) and Prof. M. J. Rosseinsky (Liverpool University) for a sample of $Ca_{2.75}C_{60}$.

CM051341K

(24) Brown, C. M.; Taga, S.; Gogia, B.; Kordatos, K.; Margadonna, S.; Prassides, K.; Iwasa, Y.; Tanigaki, K.; Fitch, A. N.; Pattison, P. *Phys. Rev. Lett.* **1999**, *83*, 2258.

(25) Takeuchi, J.; Tanigaki, K.; Gogia, B. In *Nanonetwork Materials*; AIP Conference Proceedings, Melville, 2001; Saito, S.; Ando, T.; Iwasa, Y., Eds.; Vol. 590, p 361.